Relation between connectivity and coupling in the Chilean subduction zone: a first approach

Fernanda Martín[1], Denisse Pastén[2]

[1,2]Facultad de Ciencias, Universidad de Chile, Santiago, Chile

Key Points:

- Study of complex networks applied to earthquakes in Chile.
- The relationship between the critical exponent with the coupling of the tectonic plates in Chile.
- The relation between the critic exponent with the occurrence of earthquakes in Chile.

Corresponding author: Fernanda Martín, `fernanda.martin@ug.uchile.cl`

Abstract
A time-based complex network analysis on the seismic activity along the coast of Chile was made. The coast of Chile was divided on windows of 300 km in Latitude, from Arica up to Los Angeles. The window was moved 100 km from north to south. We built a time-based earthquake complex network, on each window and we studied a directed and undirected complex network. Assuming a self-similar data network, for the directed network we found the value of the power-law characteristic exponent γ for the connectivity probability distribution. For the directed network, we analyzed the average path length, measured through steps and meters, of the data set. For each window, we obtained a similar relation between the value of γ and the average path length. The exponents and values were evaluated for the data set with the total number of seismic events with a depth greater than 200 km and of magnitude greater than $Mw = 3.0$.

Plain Language Summary

In this work different seismic data sets measured along the Chilean coast were analyzed by time-based complex network method. We have made a space window of 300 km of longitude and it was moved from the northern zone of Chile (Arica city) up to the southern zone of Chile (Los Angeles city). In each space window a complex network was built. The probability distribution of connectivity and the Average Shortest Path Length (ASPL) were computed. The complex networks built in the space windows show a scale-free behavior, although the ASPL change its value along the Chilean coast showing a dynamic behavior. The value of the slope γ was computed for each space window and it was compared with previous measures of the average coupling of the plates involves in the origin of the seismicity in Chile (Métois et al., 2013, 2016). The comparison shows an agreement between the value of γ and the average coupling in the central zone of Chile, but against values in the northern zone of Chile and the results for the southern zone of Chile are scattered, it seems to be a relation with the occurrence of large events and not with the average coupling.

1 Introduction

Despite the long tradition of studies in seismicity, this area still remains with open questions, due to the complexity of the underlying dynamic involved in the earthquake occurrence. Although, two important laws have been established along the time, one of which is the Omori law (Utsu et al., 1995), for the temporal pattern of aftershocks. The second one is the well known Gutenberg-Richter law (Gutenberg & Richter., 1954), which expresses a relationship between frequency and magnitude. In this sense, active seismic areas of the planet are interesting regions to analyze the behavior of the earthquakes and the complexity involved in the underlying physics process.

The subduction process takes place between the Nazca tectonic plate and the South America tectonic plate. This strong interaction has caused great earthquakes along the History. In particular, almost all the long coast of Chile is located on the subduction zone between these two plates, converting Chile in a seismic active zone. This great seismic activity has motivated several studies on local seismicity in Chile (Farías et al., 2011; Huan et al., 2019; Comte & Pardo., 1991; Comte et al., 2002; Martínez-Álvarez et al., 2013; Métois et al., 2013, 2016; Pastén et al., 2016; Reyes et al., 2013; Lay et al., 2010). In this work, we are doing a first approach in order to find a relationship between critical exponents and parameters of complex networks and the physical process involved in the earthquake occurrence. From a formal point of view a complex network is a set of nodes or vertices connected via connections. A complex network has certain non-trivial statistical and topological properties that do not occur in simple networks. Research in this area has had an important development in recent years, highlighting different fields, such as Biology, communication, social relations (Albert et al., 1999; Alon, 2003; Barabási et

al., 2000; Barabási & Oltvai, 2004; Bar-Joseph et al., 2003; Centola, 2010).Taking into account the characteristics of a complex network, earthquakes can be studied as a visibility graph considering the time evolution of the magnitudes (Abe & Suzuki, 2006; Abe et al., 2011), or as a spatio-temporal distribution (Pastén et al., 2016).

In this study we analyze a seismic data set measured along the coast of Chile as a directed and undirected earthquake complex network based on the time sequence of the seismic events occurrence (Abe & Suzuki, 2006; Abe et al., 2011; Abe & Suzuki, 2004; Pastén et al., 1995; Pastén et al., 2016; Pastén et al., 2018). The complete zone is divided in windows of 300 km in Latitude (from far north to the south of Chile). We move the window 100 km from north to south and we analyze the spatial evolution of the earthquake complex network. In order to make the complex networks analysis, each window is divided into cubic cells with side size of 10 km. Each cell containing hypocenter represents a node. In the directed network, the direction of the connections is defined through the temporal sequence of the seismic events in the window. The spatial evolution of the free scale behavior of this network has been analyzed by using the method of Abe et al. (Abe & Suzuki, 2006; Abe et al., 2011; Abe & Suzuki, 2004; Pastén et al., 1995). For the undirected network we used the Dijkstra algorithm (Dijkstra, 1959) to calculate the average path length (Albert & Barabási, 2002). We follow the earthquake complex network evolution along the Chilean coast.

During the last years the coupling between Nazca plate and South American plate along the Chilean subduction zone has been studied (Métois et al., 2013, 2016). That works have identified zones with more background seismicity. The highly coupled segments usually exhibit low background seismicity. We have compared our results with the high coupling and low coupling zones described by previous works (Métois et al., 2013, 2016). The results suggest that could have a relation between coupling and the value of the critical exponent γ.

2 Seismic Data

The seismic data was measured by the National Seismological Center of Chile (Centro sismológico Nacional, CSN) (*CSN: Centro Sismológico Nacional*, 2005-2017) between January 2005 and March 2017, containing 12 years of measurements with 38 083 seismic events in the zone between 17.9° to 39.1° South Latitude and between 67.5° to 75° West Longitude, with a maximum depth of 200.0 km.

The data was collected by the National Seismological Centre (Centro Sismológico Nacional) (*CSN: Centro Sismológico Nacional*, 2005-2017) in the format date, hypocenter and magnitude. For the present study the hypocenter is used in kilometers. The Latitude is represented by the angle θ and the Longitude by the angle ϕ. The Latitude and Longitude are converted into kilometers by using the following expressions,

$$\begin{aligned} d_i^{NS} &= R(\theta_i - \theta_0), \\ d_i^{EW} &= R(\phi_i - \phi_0)\cos(\theta_{av}), \\ d_i^{z} &= z_i, \end{aligned}$$

where z_i is the depth and θ_{AV} is the average Latitude. θ_0 and ϕ_0 are the minimum values for the Latitude and Longitude, and R the radius of the earth, considered for this study as 6 370 km.

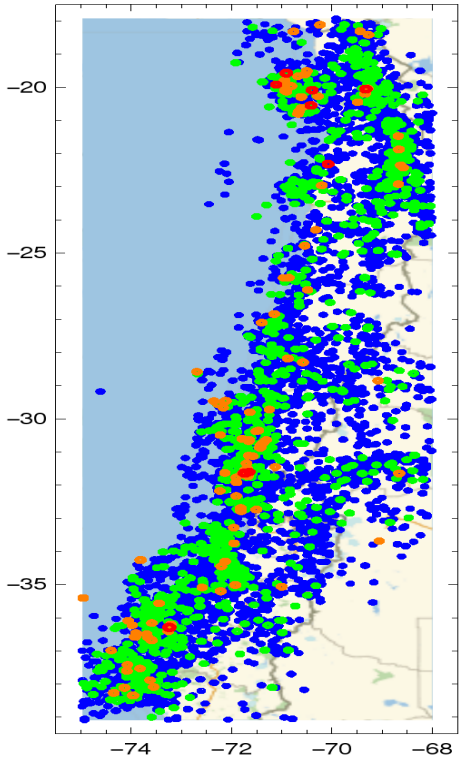

Figure 1. Map with the seismic events with magnitudes greater than $M_w = 4.0$, where the blue dots represent values of magnitude between $4.0 < M_w \leq 5.0$, the green dots is for values of magnitude between $5.0 < M_w \leq 6.0$, the orange dots for values of magnitude betweeen $6.0 < M_w \leq 7.0$ and the red ones for values of magnitude greater than $M_w = 7.0$.

2.1 Gutenberg Richter Law

Distributions of earthquakes in any region of the Earth typically satisfy the Gutenberg and Richter (Gutenberg & Richter., 1954) relationship given by

$$log_{10}(N) = a - bM, \tag{1}$$

where N is the cumulative numbers of earthquakes greater than magnitude M. The values a and b indicate the intercept and the slope of the power law. The most important parameter in this case is b, a higher value of b indicates a larger proportion of small earthquakes, and a lower value refers us to a smaller proportion of small earthquakes (Gutenberg & Richter., 1954).

3 Network Analysis

The completeness data set contains 38 083 events and it is divided in windows of 300 km in Latitude. We move the window each 100 km from the North to the South, so every window will have 200 km of the previous zone. Finally, we have $N = 22$ windows of 300 km to analyze. In order to make the time-based complex network analysis we build the network for each window, so we divide a window into cubic cells. Each cubic cell has a side size of $\Delta = 10$ km, if a hypocenter is inside the cubic cell, this cell is called as a node. In this study, two types of networks are analyzed by each window:

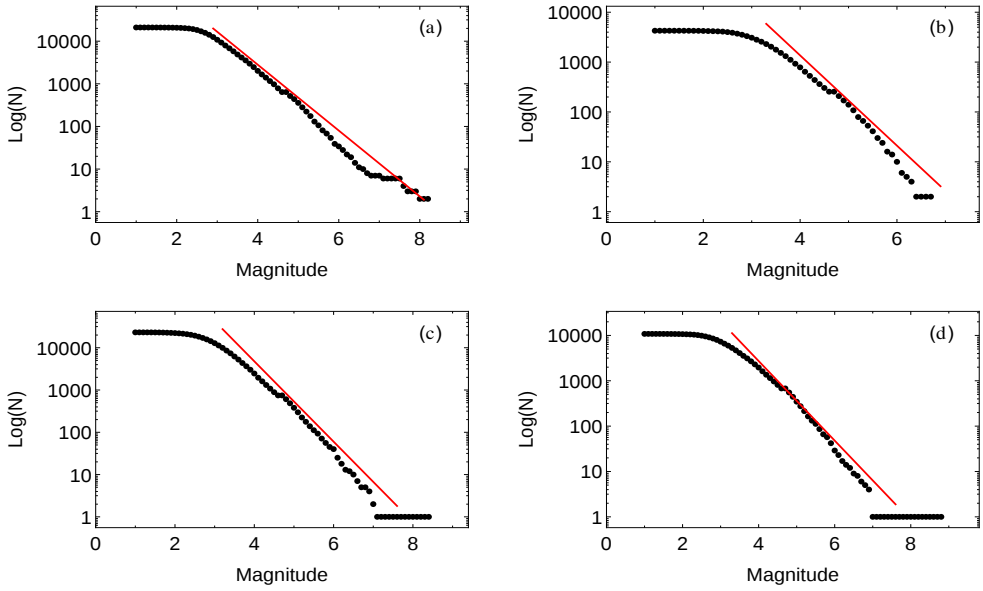

Figure 2. Complete magnitude data set is found above $M_w = 3.0$ for each zone. (a) For the area 0 km to 600 km we obtain a parameter $b = 0.77 \pm 0.01$. (b) For the area 600 km to 1200 km we obtain a parameter $b = 0.90 \pm 0.01$. (c) For the area 1200 km to 1800 km we obtain a parameter $b = 0.95 \pm 0.01$. (d) For the area 1800 km to 2400 km we obtain a parameter $b = 0.88 \pm 0.01$.

a directed and an undirected network. The connections of both types of networks depend on the earthquakes time sequence. Fig 3 shows a schematic representation of these complex networks. Each node has a mark.

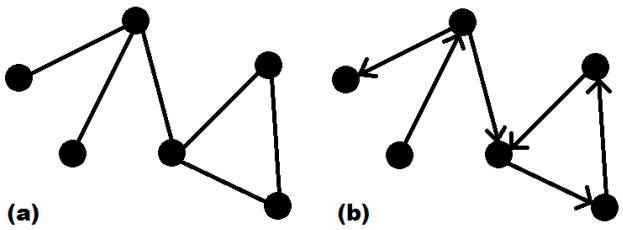

Figure 3. Schematic example of complex networks. (a) Undirected network. There is no directed edges. (b) Directed network. The edges are directed.

In the study of complex networks there are many metrics that could be useful to characterize specific systems, among them we can mention the probability distribution of connectivity ($P(k)$), the clustering coefficient (C), the betweenness centrality (σ) or the average shortest path length (l) (Newman, 2001, 2003, 2018). In the present analysis we will be concentrated in two metrics: the probability distribution of connectivity and the average shortest path length.

3.1 Probability distribution of connectivity

Generally the degree of connectivity of the nodes of a complex network is statistically distributed. In the case of time-based complex networks built with seismic data sets the probability distribution of the connectivity given by a power law (Abe & Suzuki, 2006, 2004).

$$P(k) = k^{-\gamma}, \tag{2}$$

where γ is the characteristic exponent of the scale free distribution (Telesca & Lovallo, 2012; Juan & Guzmán-Vargas, 2013).That fact shows a scale-free behavior of the seismicity in the distribution of the connectivity. We follow this behavior window by window along the Chilean coast in the subduction zone of Chile, so we show a spatial evolution of the γ exponent. In order to obtain a reliable value of the γ exponent, we have used two different methods to evaluate γ: the linear regression and the Maximum Likelihood Estimation (MLE) and we compare both results by each window, it is due to the fact that some areas have a small number of points (seismic events).

The MLE is computed by using the approximation proposed by (Goldstein et al., 2004) for discrete data with a scale-free distribution, and the range of application used is determined by for Kolgomorov-Smirnov test. On the other hand a Linear Regression analysis is made on the histogram obtained from the log-log probability distribution of connectivity of the complex network. The LR analysis was applied to the same range used in the MLE analysis.

Figs.4 and 5 show the linear range of the probability distribution of connectivity by using the two methods LR and MLE for each window, from the far north of Chile to the south of Chile. We can remark that both methods fit very well the power law in the same linear range along the coast of Chile. In some windows, like windows 7, 8 , 9 , 10, 21 and 22 (Figs. 4g), 4h), 4i), 4j), 5i), 5j)), the number of seismic events measured is smaller than the number of seismic events in the other windows, that is due the number of seismic station in those zones is less than the other zones, but value of the adjustment obtained with the two methods is very similar. The spatial evolution of the time-based complex network is shown in Fig. 6, where the value of the critical exponent γ is calculated by Latitude. This figure is showing the change of this exponent along the subduction zone.

3.2 Average Shortest Path Length (ASPL)

The Average Shortest Path Length (ASPL) is a useful metric that considers the distance between nodes inside the network (Newman, 2001, 2003, 2018). First, we will measure the distance between all the nodes in the network following the path of connections.

The distance between nodes in the network will be determinated by measuring the distance from the center of a node to the center of one of the nodes connected to it. The APSL is a concept in network topology that is defined as the average number of steps along the shortest paths for all possible pairs of nodes in the network. It is a measure of the efficiency of the information transference or mass transport on a network, and it is given by

$$ASPL = \frac{1}{n(n-1)} \dot{\sum}^{i\ j} d(v_i, v_j). \tag{3}$$

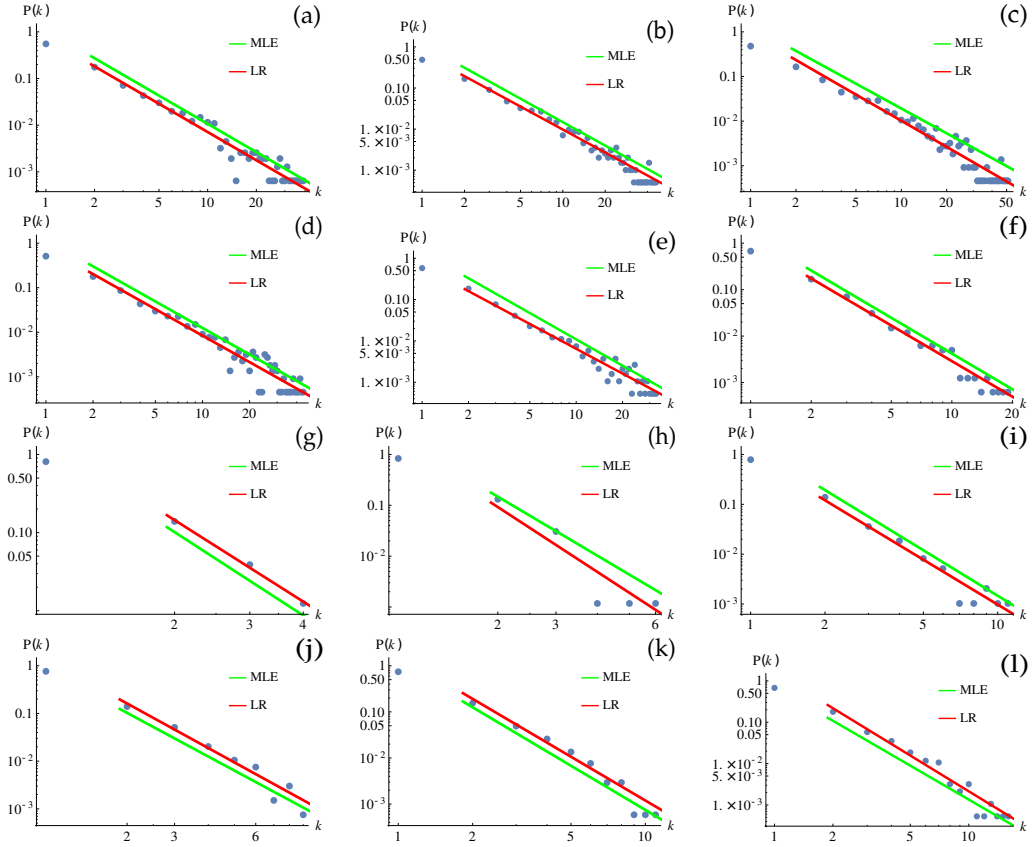

Figure 4. Maximum Likelihood Estimation (MLE) and Linear regression (LR) for the probability distribution of connectivity in each of the first 12 windows used in this analysis. From the north to the south of Chile: a) 0 km to 300 km, b) 100 km to 400 km, c) 200 km to 500 km, d) 300 km to 600 km, e) 400 km to 700 km, f) 500 km to 800 km, g) 600 km to 900 km, h) 700 km to 1000 km, i) 800 km to 110 km, j) 900 km to 1200 km, k) 1000 km to 1300 km, l) 1100 km to 1400 km.

Here n denotes the total number of nodes in the network and $d(v_i, v_j)$ is the value of shortest-path length of nodes v_i and v_j. The $d(v_i, v_j)$ has been calculated with the Dijkstra algorithm (Dijkstra, 1959).

Fig. 8 shows the values of the ASPL for the complex network built in each window studied. This value is calculated by steps in the network, i.e., how many steps are between two nodes (blue points) and by the euclidean distance between nodes, considering the distance in kilometers from the center of a node to the center of the another node (red points). Both measurements have a similar general behavior. The values of the ASPL are very similar along the Chilean coast, except for the regions that contain a smaller number of seismic events.

3.3 Spearman Rank Correlation

Spearman rank correlation is a non-parametric test that is used to measure the degree of association between two variables (Lyerly, 1952; Fieller et al., 1957). The Spear-

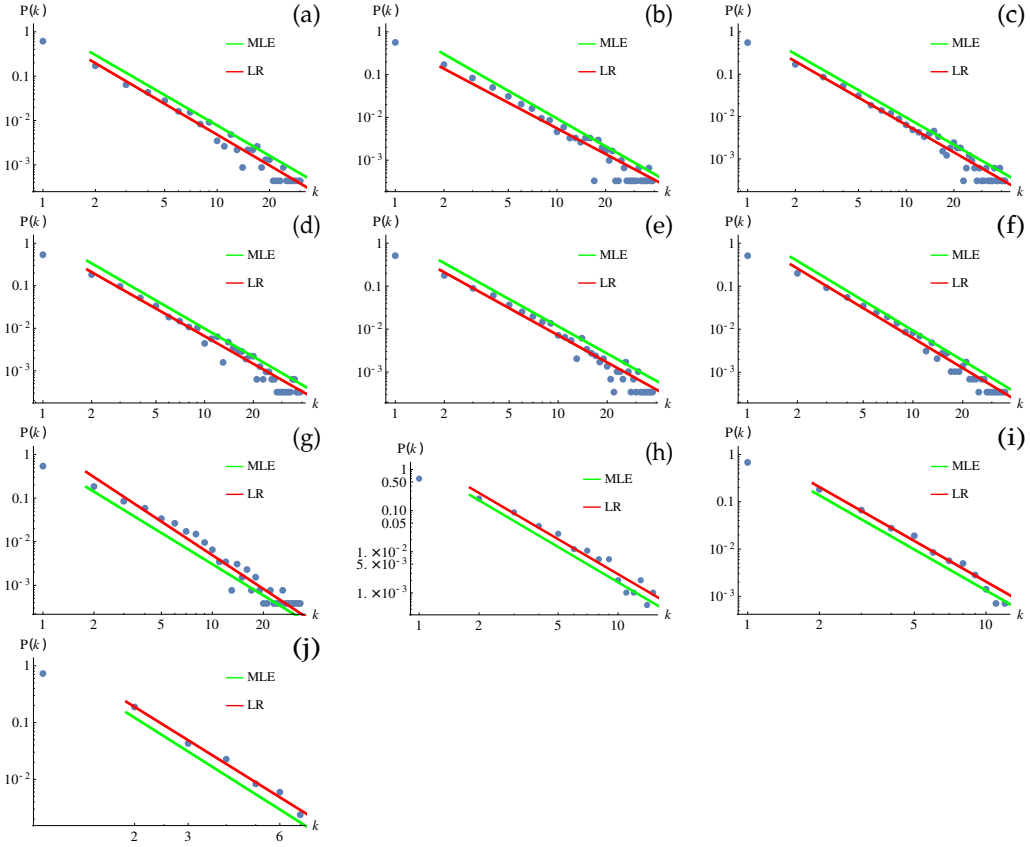

Figure 5. Maximum Likelihood Estimation (MLE) and Linear regression (LR) for the probability distribution of connectivity of the 10 last windows used in this analysis. From the north to the south of Chile: a) 1200 km to 1500 km, b) 1300 km to 1600 km, c) 1400 km to 1700 km, d) 1500 km to 1800 km, e) 1600 km to 1900 km, f) 1700 km to 2000 km, g) 1800 km to 2100 km, h) 1900 km to 2200 km, i) 2000 km to 2300 km, j) 2100 km to 2400 km.

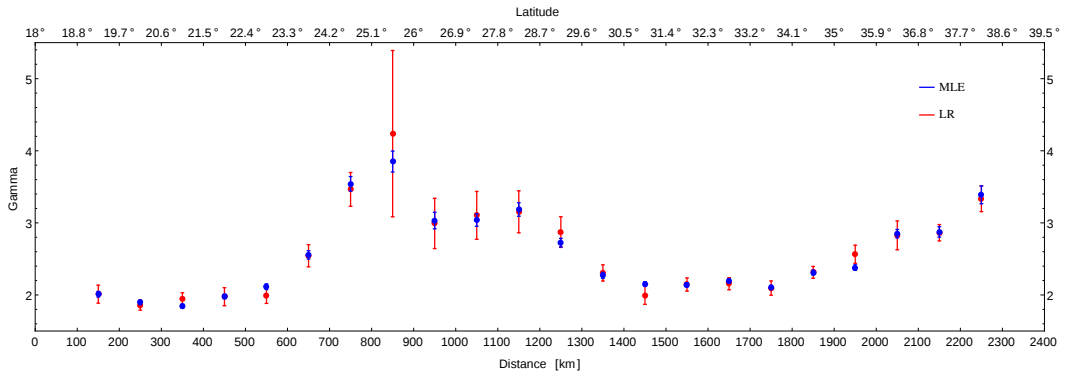

Figure 6. Value of γ along the Chilean coast. From the 18° to the 39° South Latitude.

man correlation coefficient, ρ, can take values in a range between $[-1,\ 1]$. When ρ has the value 1 it indicates a perfect association of ranks, when the value of ρ is zero it indicates no association between ranks and when the value of ρ is -1 it indicates a perfect negative association of ranks. The following formula shows how this coefficient is

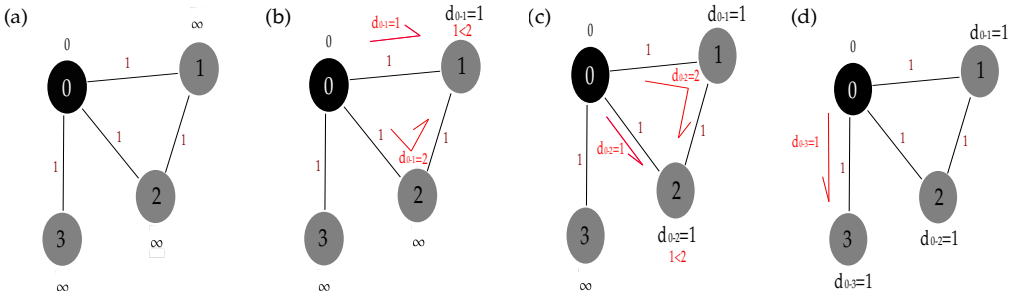

Figure 7. Schema of the method to calculate the shortest path length, through Dikjstra Algorithm. (a) The initial network, where the values of the shortest path length between all the nodes and the initial node (0) is infinity. (b) It is calculated the shortest path length between the initial node and the node 1. Two paths were found and are compared one another the shortest path replaces the distance infinity, and is defined like the shortest path between the node 0 and the node 1. (c) The same process done with node 1 is done with node 2. (d) And finally the process is ended with the last node.

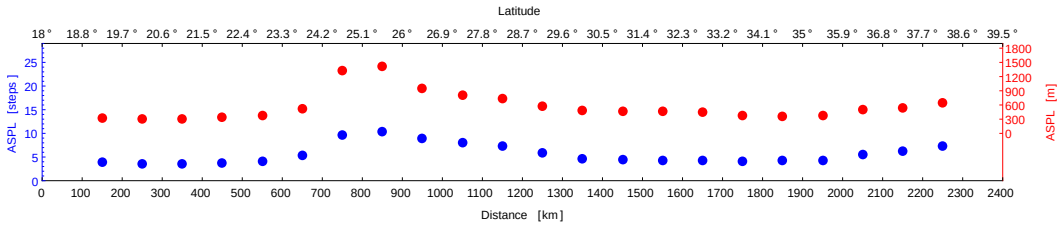

Figure 8. Average Shortest Path Lenght (ASPL) calculated for each window along the Chilean coast, from the northern zone to the southern zone of Chile. This value was calculated by kilometers and by steps in the network.

calculated

$$\rho = 1 - \frac{6\sum_i d_i^2}{n(n-1)},$$

where d_i is the difference between ranks and n is the number of observations.

Finally, Fig. 11 is showing the longitude of the rupture zone for three large earthquakes occurred along Chilean coast in the last 10 years.

4 Discussion

We have characterized the seismicity along the coast of Chile by using a time-based complex network description. We have divided the coast from the northern to the southern of Chile in windows of 300 km and we have applied the time-based complex network method in each window. Windows are divided into cubic cells and each node corresponds to a cubic cell with at least one hypocenter inside of it. In this analysis we have followed the spatial evolution along the Chilean coast of two parameters of complex networks: the critical exponent γ (probability distribution of connectivity) and the ASPL.

Fig. 6 shows the values of γ along the Chilean subduction zone. These values are calculated by using two different methods the Linear Regression (LR) and the Maximum Likelihood Estimation (MLE). This figure shows the comparison of these two methods,

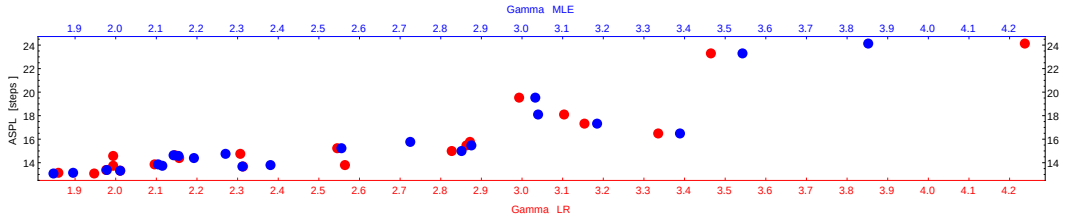

Figure 9. Average Path Length for each value versus the critical exponent γ, calculated by a simple Linear Regression (LR) and the Maximum Likelihood Estimation method (MLE).

	Average Coupling	γ_{MLE}
γ_{LR}	0.191417	0.979673
γ_{MLE}	0.218521	1

Table 1. Spearman Rank correlation coefficient between the values of the exponent γ, previously calculated using the linear regression and the Maximum Likelihood Estimation (MLE), and the values of Average Coupling from Métois paper's (Métois et al., 2013, 2016). The values shown are seen in figures 9, 10 and 11.

Latitude S	Average Coupling
18.8° - 23.3°	−0.9
23.3° - 32.3°	0.636364
32.3° - 38.8°	0.142857

Table 2. Spearman Rank correlation coefficient between the values of the exponent γ, previously calculated using the Maximum Likelihood Estimation (MLE), and the values of Average Coupling from Métois paper's, separated into different zones. The values shown are seen in figure 11.

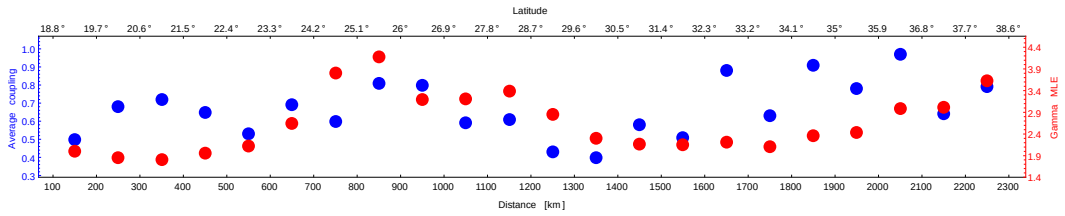

Figure 10. Average coupling obtained by Metóis et al. (Métois et al., 2013, 2016) versus the critical exponent γ calculated with the Maximum Likelihood Estimation method (MLE).

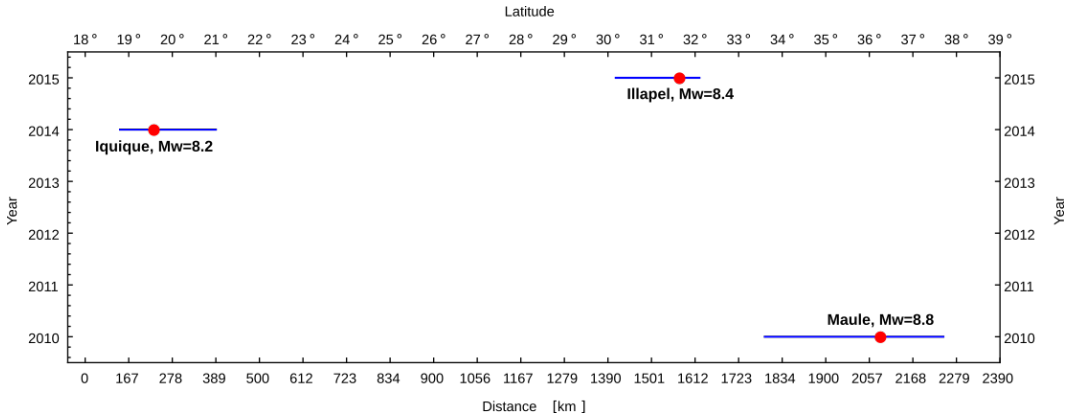

Figure 11. Longitude of the rupture zone of the last three large earthquakes occurred in Chile, M_w8.8 Maule (2010), M_w8.2 Iquique (2014) and M_w8.3 Illapel (2015).

presenting a good agreement between both results. The values of the Spearman Rank shown in Table 1 supports this agreement.

Fig. 8 shows the evolution of the Average Shortest Path Length (ASPL) along the Chilean coast. This figure compares the values measured by steps in the network and the Euclidean distance measured in kilometers, both measures show a good agreement in the ASPL. On the other hand, Fig. 9 show the ASPL versus the values of γ calculated by LR (red) and MLE (blue). This two metrics, the ASPL and the critical exponent γ, show a good correlation along the zone studied. In order to evaluate the correlation between this two metrics, Table 1 shows the Spearman Rank value for Fig. 9.

In order to make a first approach to the physical dynamics of earthquakes and the complex networks parameters, we have compared the critical exponent γ against the coupling in the coast of Chile. For this purpose, we have taken the results of Metois et al. (Métois et al., 2013, 2016), who measured the coupling along Chilean coast. Fig. 10 shows a good correlation between the values of γ and the coupling in the central zone of Chile between these two parameters, while there is not a good correlation in the northern zone and in the southern zone. Table 2 shows the Spearman rank correlation for this figure, the best correlation is obtained for the central zone of Chile.

5 Concluding Remarks

Two time-based a directed and undirected complex networks are constructed for a data set measured along the coast of Chile, network. We compute the values of the characteristic exponent γ (from the probability distribution of connectivity) for the directed network, and we compute the Average Shortest Path Length (ASPL) for the undirected network.

This study shows a change in the behavior of the value of γ and the values of the Average Path Length, for each zone under study. Both of these values are not constant along the Chilean subduction zone. The value of γ increases between the 23.3° and the 29.6° South Latitude, the value of this parameter keeps in a vale in the northern zone of Chile (between 18.5° and 23.2° South Latitude). The last large earthquake in the northern zone of Chile was on 1st April 2014, with a moment mangnitude of M_w8.2 and broken a fault region of 150 km, which is shown in Fig. 11. There seems to be a correlation between a low value of γ and the rupture zone in Iquique.

On 16th September 2015, a large earthquake with moment magnitude of $M_w 8.3$ occurred close to the Illapel city, located at 31.6° South Latitude, with epicenter in 31.5° South Latitude and a fault zone of 200 km, aprox, to the north of the epicenter. In the spatial vicinity of this two large earthquakes we compute a low value of γ, this fact is in agreement with the recent past occurrence of large earthquakes on these two zones.

The capital of Chile, Santiago, is located at 33.47° South Latitude, the zone around the capital shows a low value of γ. The values of this parameter grows again from the 35° South Latitude. The Maule 2010 large earthquake had the epicenter at 36.2° South Latitude, with a moment magnitude of $M_w 8.8$. In the vicinity of the zone affected by this large earthquake the value of γ is increasing. Following the spatial evolution of the critical exponent γ and the ASPL, it seems that the spatial evolution of the parameter γ has a good agreement with the large earthquake occurrence, so γ could be an indicator that could show the behavior of the physical dynamic involved in the earthquake occurrence. The agreement of this parameter with the coupling zones is high, see in Table 1, the highest coupling zones, according Metois (Métois et al., 2013, 2016), have a value of γ closed to 2, and the Low coupling zones have a value of γ greater than 3. In addition, Fig. 11 shows a great agreement between the low values of γ and the large earthquake occurrence. This is a first effort to connect parameters of complex networks with the physical dynamic of earthquakes occurrence.

6 Open Research

The data is available for future research in the research data repository of the University of Chile (Martín & Pastén, 2020a, 2020b).

Acknowledgments
The researchers of this study thank the National Seismological Center of Chile (*CSN: Centro Sismológico Nacional*, 2005-2017) for the data provided.

References

Abe, S., Pastén, D., Muñoz, V., & Suzuki, N. (2011). *Universalities of earthquake-network characteristics. Chinese Science Bulletin*, ***56***, 34. doi: https://doi.org/10.1007/s11434-011-4767-6

Abe, S., & Suzuki, N. (2004). *Scale-free network of earthquakes. Chinese Science Bulletin*, ***65***, 581. doi: https://doi.org/10.1209/epl/i2003-10108-1

Abe, S., & Suzuki, N. (2006). *Complex-network description of seismicity. Nonlinear Proc. Geophys*, ***13***, 145-150. doi: https://doi.org/10.5194/npg-13-145-2006

Albert, R., & Barabási, A. L. (2002). *Statistical mechanics of complex networks. Reviews of modern physics.*, ***74***, 47. doi: https://doi.org/10.1103/RevModPhys.74.47

Albert, R., Jeong, H., & Barabasi., L. (1999). *Diameter of the world wide web. Nature.*, ***401***, 130-131. doi: https://doi.org/10.1038/43601

Alon, U. (2003). *Biological networks: the tinkerer as engineer. Science.*, ***301***, 1866–1867. doi: https://doi.org/10.1126/science.1089072

Barabási, A., Albert, R., & Jeong, H. (2000). *Scale-free characteristics of random networks: the topology of the world-wide web. Physica A: Statistical Mechanics and its Applications.*, ***281***, 69-77. doi: https://doi.org/10.1016/S0378-4371(00)00018-2

Barabási, A., & Oltvai, Z. N. (2004). *Network biology: understanding the cell's functional organization. Nature Reviews Genetics.*, ***5***, 101–113. doi: https://doi.org/10.1038/nrg1272

Bar-Joseph, Z., Gerber, G. K., Lee, T. I., Rinaldi, N. J., Yoo, J. Y., Robert, F.,

... Gifford, D. K. (2003). *Computational discovery of gene modules and regulatory networks. Nature Biotechnologyvolume.*, ***21***, 1337–1342. doi: https://doi.org/10.1038/nbt890

Centola, D. (2010). *The Spread of Behavior in an Online Social Network Experiment. Science.*, ***329***, 1194-1197. doi: https://doi.org/10.1126/science.1185231

Comte, D., Haessler, H., Dorbath, L., Pardo, M., Monfret, T., Lavenu, A., ... Hello, Y. (2002). *Seismicity and stress distribution in the Copiapo, northern Chile subduction zone using combined on- and off-shore seismic observations. Physics of the Earth and Planetary Interiors.*, ***132***, 197-217. doi: https://doi.org/10.1016/S0031-9201(02)00052-3

Comte, D., & Pardo., M. (1991). *Reappraisal of great historical earthquakes in the northern Chile and southern Peru seismic gaps. Natural Hazards.*, ***4***, 23-44. doi: https://doi.org/10.1007/BF00126557

Csn: Centro sismológico nacional. (2005-2017). https://www.sismologia.cl/.

Dijkstra, E. W. (1959). *A Note on Two Problems in Connexion with Graphs. Numerische Mathematik.*, ***1***, 269-271. doi: https://doi.org/10.1007/BF01386390

Farías, M., Comte, D., Roecker, S. W., Carrizo, D., & Pardo, M. (2011). *Crustal extensional faulting triggered by the 2010 Chilean earthquake: The Pichilemu Seismic Sequence. Tectonics*, ***30***. doi: https://doi.org/10.1029/2011TC002888

Fieller, E. C., Hartley, H. O., & Pearson, E. S. (1957). *Tests for Rank Correlation Coefficients. I. Biometrika.*, ***44***, 470-481. doi: https://doi.org/10.2307/2332878

Goldstein, M. L., Morris, S., & Yen, G. G. (2004). *Problems with fitting to the power-law distribution. . The European Physical Journal B.*, ***41***, 255-258. doi: https://doi.org/10.1140/epjb/e2004-00316-5

Gutenberg, B., & Richter., C. (1954). *Seismicity of the earth and associated phenomena.* (N. . P. U. P. Princeton, Ed.).

Huan, Z., Tilmann, F., Comte, D., & Zhao., D. (2019). *P Wave Azimuthal Anisotropic Tomography in Northern Chile: Insight Into Deformation in the Subduction Zone. Journal of Geophysical Research Solid Earth.*, ***124***, 742-765. doi: https://doi.org/10.1029/2018JB016389

Juan, B. A.-S., & Guzmán-Vargas, L. (2013). *Earthquake magnitude time series: scaling behavior of visibility networks. . The European Physical Journal B.*, ***86***, 454. doi: https://doi.org/10.1140/epjb/e2013-40762-2

Lay, T., Ammon, C. J., Kanamori, H., Koper, K. D., , Sufri, O., & Hutko, A. R. (2010). *Teleseismic inversion for rupture process of the 27 February 2010 Chile (Mw 8.8) earthquake. Applied Soft Computing.*, ***37***. doi: https://doi.org/10.1029/2010GL043379

Lyerly, S. B. (1952). *The average spearman rank correlation coefficient. Psychometrika.*, ***17***, 421-428. doi: https://doi.org/10.1007/BF02288917

Martín, F., & Pastén, D. (2020a). Replicar los datos para: Data set of seismology of chile (2005-2017). doi: https://doi.org/10.34691/FK2/VENURN

Martín, F., & Pastén, D. (2020b). Replicar los datos para: Relation between connectivity and coupling in the chilean subduction zone: a first approach: Figures and tables. doi: https://doi.org/10.34691/FK2/C3X8AE

Martínez-Álvarez, F., Reyes, J., Morales-Esteban, A., & Escudero, C. R. (2013). *Determining the best set of seismicity indicators to predict earthquakes. Two case studies: Chile and the Iberian Peninsula. Physics of the Earth and Planetary Interiors.*, ***50***, 198-210. doi: https://doi.org/10.1016/j.knosys.2013.06.011

Métois, M., Socquet, A., Vigny, C., Carrizo, D., Peyrat, S., Delorme, A., ... Ortega, I. (2013). *Revisiting the North Chile seismic gap segmentation using GPS-derived interseismic coupling. Geophys. J. Int.*, ***194***, 1283-1294. doi:

https://doi:10.1093/gji/ggt183

Métois, M., Vigny, C., & Socquet, A. (2016). *Interseismic coupling, megathrust earthquakes and seismic swarms along the Chilean subduction zone (38–18 S). Pure and Applied Geophysics.*, ***173***, 1431-1449. doi: https://doi.org/10.1007/s00024-016-1280-5

Newman, M. E. J. (2001). *Scientific collaboration networks. II. Shortest paths, weighted networks, and centrality. Physical Review Journals.*, ***64***. doi: https://doi.org/10.1103/PhysRevE.64.016132

Newman, M. E. J. (2003). *The Structure and Function of Complex Networks. Society for Industrial and Applied Mathematics.*, ***45***, 167-256. doi: https://doi.org/10.1137/S003614450342480

Newman, M. E. J. (2018). *Networks Second Edition.* (U. P. Oxford, Ed.).

Pastén, D., Abe, S., Muñoz, V., & Suzuki., N. (1995). *Scale-free and small-world properties of earthquake network in Chile. arXiv preprint arXiv:1005.5548*, ***43***, 1-33. doi: https://doi.org/10.4294/jpe1952.43.1

Pastén, D., Czechowski, Z., & Toledo, B. (2018). *Time series analysis in earthquake complex networks. Chaos: An Interdisciplinary Journal of Nonlinear Science.*, ***28***. doi: https://doi.org/10.1063/1.5023923

Pastén, D., Torres, F., Toledo, B., Muñoz, V., Rogan, J., & Valdivia, J. A. (2016). *Time-Based Network Analysis Before and After the M w 8.3 Illapel Earthquake 2015 Chile. Pure and Applied Geophysics.*, ***173***, 2267-2275. doi: https://doi.org/10.1007/s00024-016-1335-7

Reyes, J., Morales-Esteban, A., & Martínez-Álvarez, F. (2013). *Neural networks to predict earthquakes in Chile. Applied Soft Computing.*, ***13***, 1314-1328. doi: https://doi.org/10.1016/j.asoc.2012.10.014

Telesca, L., & Lovallo, M. (2012). *Analysis of seismic sequences by using the method of visibility graph. . Europhysics Letters.*, ***97***(5). doi: https://doi.org/10.1209/0295-5075/97/50002

Utsu, T., Ogata, Y., & Matsu'ura., R. S. (1995). *The Centenary of the Omori Formula of a Decay Law for Aftershock Activity. Journal of Physics of the Earth*, ***43***, 1-33. doi: https://doi.org/10.4294/jpe1952.43.1